

# Quinacrine reactivity with prion proteins and prion-derived peptides

Zbigniew Zawada · Martin Šafařík · Eva Dvořáková · Olga Janoušková · Anna Březinová · Ivan Stibor · Karel Holada · Petr Bouř · Jan Hlaváček · Jaroslav Šebestík

Received: 13 July 2012 / Accepted: 5 January 2013 / Published online: 23 January 2013  
© Springer-Verlag Wien 2013

**Abstract** Quinacrine is a drug that is known to heal neuronal cell culture infected with prions, which are the causative agents of neurodegenerative diseases called transmissible spongiform encephalopathies. However, the drug fails when it is applied in vivo. In this work, we analyzed the reason for this failure. The drug was suggested to “covalently” modify the prion protein via an acridinyl exchange reaction. To investigate this hypothesis more closely, the acridine moiety of quinacrine was covalently attached to the thiol groups of cysteines belonging to prion-derived peptides and to the full-length prion protein. The labeled compounds were conveniently monitored by fluorescence and absorption spectroscopy in the ultraviolet and visible spectral regions. The acridine

moiety demonstrated characteristic UV–vis spectrum, depending on the substituent at the C-9 position of the acridine ring. These results confirm that quinacrine almost exclusively reacts with the thiol groups present in proteins and peptides. The chemical reaction alters the prion properties and increases the concentration of the acridine moiety in the prion protein.

**Keywords** Quinacrine · Prion protein and peptide model reactions · Solid phase and recombinant synthesis

## Introduction

The 9-aminoacridines are an important class of compounds in medicine used for the treatment of cancer, viruses and neurodegenerative diseases. The biological activities of peptides and proteins can be modified by conjugation with these compounds. (Demeunynck et al. 2001; Šebestík et al. 2007; Wallace 1989; Korth et al. 2001; Denny 2003; May et al. 2003; Eiter et al. 2009; Goodell et al. 2008; Rosini et al. 2008; Rodriguez-Franco et al. 2006; Guddneppanavar et al. 2006). Among 9-aminoacridines, quinacrine (6-chloro-9-(4-(*N,N*-diethylamino)-1-methylbutylamino)-2-methoxyacridine) is perhaps the most important drug. It is used for the treatment of various diseases such as *rheumatoid arthritis*, *lupus erythematosus*, chloroquine-resistant malaria, tapeworm infections (*Taenia saginata*), Chagas disease, and epilepsy (refractory *petit mal*) (Wallace 1989; Korth et al. 2001; Krauth-Siegel et al. 2005; Saravanamuthu et al. 2004; Wild and Young 1965; Burnett et al. 2003). Quinacrine can act on multiple cellular targets. Quinacrine inhibits DNA and RNA polymerases, suppresses prostaglandin synthesis, stabilizes neutrophils and lysosomes, and serves as an antagonist of the bradykinin

**Electronic supplementary material** The online version of this article (doi:10.1007/s00726-013-1460-x) contains supplementary material, which is available to authorized users.

Z. Zawada · M. Šafařík · A. Březinová · I. Stibor · P. Bouř · J. Hlaváček (✉) · J. Šebestík (✉)  
Institute of Organic Chemistry and Biochemistry,  
Academy of Sciences of the Czech Republic,  
Flemingovo nám. 2, 166 10 Prague 6, Czech Republic  
e-mail: honzah@uochb.cas.cz

J. Šebestík  
e-mail: jsebestik@seznam.cz

Z. Zawada  
Institute of Chemical Technology, Technická 5,  
166 28 Prague 6, Czech Republic

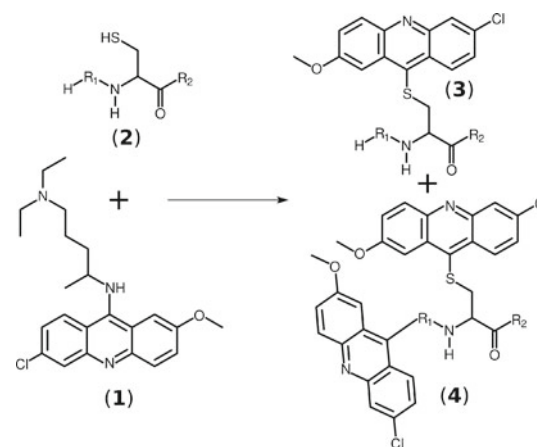
E. Dvořáková · O. Janoušková · K. Holada  
First Faculty of Medicine, Charles University in Prague,  
Studničkova 7, 128 00 Prague 2, Czech Republic

I. Stibor  
Technical University of Liberec, Studentská 2,  
461 17 Liberec 1, Czech Republic

and histamine receptors (Wallace 1989). The anticancer activity of quinacrine is attributed to its inhibition of the binding between a BH3 domain-derived peptide and the anti-apoptotic protein Bcl-xL (Orzáez et al. 2009).

We chose to study the binding of this drug to model molecules to understand the affinity of the 9-aminoacridines for peptides in more detail (Fig. 1). Since quinacrine reduces the propagation of prions (PrP<sup>ts</sup>) in cell culture, this drug could serve as a potential anti-prion agent for the treatment of patients with Creutzfeldt–Jakob disease or the new variant of this disease (Korth et al. 2001). Indeed, several bis-acridinylated compounds have been tested for their anti-prion activity (May et al. 2003). The minimal distance between amino groups that was required to obtain a synergistic effect between the two 9-aminoacridine units in highly active compounds was 10 Å. A similar effect of bis-acridinylated compounds was also observed on the inhibition of acetylcholinesterase-catalyzed aggregation of Aβ1-40, which is involved in Alzheimer's disease (Bolognesi et al. 2007). A sufficient improvement of the anti-prion activity of quinacrine was achieved using a chimeric ligand approach, which resulted in a 20 nM prion inhibitor (Dollinger et al. 2006). Recently, it has been shown that quinacrine and a γ-secretase inhibitor prevent dendritic degeneration in murine brains by reducing the PrP<sup>Sc</sup> levels (Spilman et al. 2008). Although quinacrine demonstrated excellent in vitro results (Korth et al. 2001), in clinical trials with a dosage of 300 mg per day, no significant effect on the course of prion disease was observed (Collinge et al. 2009). In a murine model of Creutzfeldt–Jakob disease, quinacrine did not prolong survival (Collins et al. 2002). This result cannot be explained by low bioavailability, because quinacrine reached a sufficient brain concentration 1,500 ng/g in mice with an average dosing of 56 mg/kg/day after 4 weeks (Yung et al. 2004). The lack of in vivo efficacy was hypothesized to be due to an accumulation of quinacrine-resistant prion conformations (Ghaemmaghami et al. 2009). Thus, a better understanding of the role of quinacrine in the in vitro assay could lead to a new drug that will be active in vivo.

We have previously suggested that the discrepancy between the anti-prion activity of quinacrine (EC<sub>50</sub> 0.3 μM; Korth et al. 2001; May et al. 2003) and its low affinity to PrP (K<sub>d</sub> 4.6 mM; Vogtherr et al. 2003) could be attributed to the covalent attachment of acridine moieties to the ε-amino groups of lysine residues in peptides and proteins leading to the subsequent accumulation of the hydrophobic acridine moiety (Šebestík et al. 2006). In an aqueous environment, this reaction is limited to amines with low pK<sub>a</sub> and is accompanied by hydrolysis to the corresponding acridones (Kunikowski and Ledochowski 1981; Paul and Ladame 2009). On the other hand, strong nucleophiles such as NH<sub>2</sub>OH (Schantl and Turk 1990), Ph-NHNH<sub>2</sub> (Wysocka-Skrzela 1986), and thiols (Wild and Young 1965;



R <sub>1</sub>	R <sub>2</sub>	#
-Asp-	-Val-Asn-OH	<b>2a, 3a, 4a</b>
-His-Asp-	-Val-Asn-OH	<b>2b, 3b, 4b</b>
-Thz-His-Asp-	-Val-Asn-OH	<b>2c, 3c</b>
-Glu-Gln-Met-	-Ile-Thr-Asn-OH	<b>2d, 3d, 4d</b>
-Glu-Gln-Met-	-Val-Thr-Asn-OH	<b>2e, 3e, 4e</b>
-γ-Glu-	-Gly-OH	<b>2h, 3g, 4h</b>

**Fig. 1** Transfer of the aromatic moiety of quinacrine (1) to cysteine residues (2) of prion-derived peptides. An acridine moiety covalently attached to a Cys residue is referred to as Cys(Qui) in this work (3). In some cases, acridinylation at the N-terminus can also occur (4). The sequences for proteins **2f**, **2g**, **3f**, **4f** and **4g** are detailed in the “Materials and methods”

Weltrowski et al. 1982) can react with 9-aminoacridines even at physiological conditions. The thiol groups of cysteine and glutathione can serve as acridine moiety acceptors. Taking into account the higher nucleophilicity of sulfur atoms relative to nitrogen atoms (Wild and Young 1965), we focused our attention on the prion cysteines as the possible acceptors of the acridine moiety of quinacrine (Fig. 1) and attempted to covalently label the SH groups of prion proteins and prion-derived peptides with quinacrine. The Cys(Qui) abbreviation is used to represent a cysteine residue with an acridine moiety covalently attached to its SH group. Preliminary studies were presented at the 31st European Peptide Symposium (Zawada et al. 2010).

## Materials and methods

### General methodologies

Wang resin was purchased from Bachem (Bubendorf, Switzerland). Other commercially available chemicals

including Fmoc-amino acids were purchased from Merck, Sigma-Aldrich Corporation and Fluka (Prague, Czech Republic) and were used without further purification. The products were dried in a vacuum drying box (Salvis AG, Emmenbrücke, Luzern, Switzerland) at room temperature for 16 h. During the syntheses, the molecular weights of the peptide fragments were determined using matrix assisted laser desorption ionization and electrospray ionization mass spectrometries (MALDI-TOF-MS and ESI-MS; Bruker Daltonics Reflex IV and Waters Q-ToF micro instruments, respectively). The  $^1\text{H-NMR}$  and  $^{13}\text{C-NMR}$  spectra were measured on a Bruker Avance II<sup>TM</sup> 600 MHz spectrometer equipped with Cryoprobe (Bruker Biospin AG, Fällanden, Switzerland). Agilent 1200 instrument (Santa Clara, CA, USA) with a quaternary pump, thermostat, diode array detector and a reversed-phase C<sub>18</sub> columns were used for HPLC. The peptides were purified by semipreparative HPLC on a VYDAC 250 × 10 mm, 10 μm Vydac RP-18 column (The Separations Group, Hesperia, CA, USA) with a flow rate of 3 mL/min and a gradient (Gr) of 0–100 % acetonitrile (ACN) in 0.05 % aqueous trifluoroacetic acid (TFA). The analytical HPLC parameters are summarized in Table 1. The HPLC purity of the prepared peptides was greater than 95 %.

UV-vis spectra were acquired using a Varian Carry 5000 instrument (Palo Alto, CA, USA) with a quartz cell (1 cm). Savitzky and Golay smoothing was applied to the protein-bound acridine spectrum (Savitzky and Golay 1964; Steinier et al. 1972; Madden 1978). For comparison, the same procedure was applied to the unmodified and modified proteins (Fig. 2 spectra (f) and (g), respectively).

Fluorescence measurements were carried out using a Jasco FP-6600 instrument with an excitation wavelength of 269 nm. The spectra (Fig. 3; Table 3) were fitted using the Edgeworth-Cramer peak function (Dondi 1982).

Syntheses of peptides 2a–2f using methods A and B

The peptides were synthesized using the Fmoc/tBu procedure (Fields and Noble 1990) either manually (2a–2e, method A) or with an automatic solid-phase peptide synthesizer ABI 433A (Applied Biosystems) (2f, method B).

#### Method A

Wang resin (1.000 mg, a substitution of 1.1 mmol g<sup>-1</sup>) was loaded with a mixture of Fmoc-Asn(Trt)-OH (5 eq), DIC (5.5 eq) and DMAP (0.25 eq) in DMF for 17 h. A final loading of 0.4 mmol g<sup>-1</sup> was determined from the absorbance of dibenzofulvene at 301 nm (Meienhofer et al. 1979; Chang et al. 1980). The remaining unreacted hydroxyl group was capped with Ac<sub>2</sub>O (1 eq) and TEA (1.2 eq) in DMF for 1 h. The resin was split into five portions (ca. 200 mg) and peptides 2a–2e were synthesized using Fmoc-protected amino acids (4 eq), HOBt (4.2 eq) and DIC (4.5 eq) in DMF. The progress of each peptide coupling reaction was monitored by ninhydrin (Kaiser et al. 1970; Sarin et al. 1981), chloranil (Vojtkovský 1995) or bromophenol blue tests (Krchňák et al. 1988a, b). Fmoc deprotection was monitored by the precipitation of dibenzofulvene in water. Peptides were cleaved from the resin with a TFA:H<sub>2</sub>O:EDT:TIS (94:2.5:2.5:1) mixture for 3 h. The solvent was evaporated under a stream of nitrogen and the residue was precipitated with cold Et<sub>2</sub>O. The synthesized peptides were purified by preparative HPLC.

Obtained peptides:

**MoPrP177-180**—H-Asp-Cys-Val-Asn-OH (2a)—HPLC RT (Gr 1) 10.6 min. For C<sub>16</sub>H<sub>27</sub>N<sub>5</sub>O<sub>8</sub>S (449.16) found ESI-MS, *m/z*: 450.2 (M+H<sup>+</sup>).

**MoPrP178-213**—H-His-Asp-Cys-Val-Asn-OH (2b)—HPLC RT (Gr 1) 11.4 min. For C<sub>22</sub>H<sub>34</sub>N<sub>8</sub>O<sub>9</sub>S (586.22) found ESI-MS, *m/z*: 587.2 (M+H<sup>+</sup>).

**[Thz<sup>175</sup>]MoPrP175-180**—H-Thz-His-Asp-Cys-Val-Asn-OH (2c)—HPLC RT (Gr 2) 7.0 min. For C<sub>26</sub>H<sub>39</sub>N<sub>9</sub>O<sub>10</sub>S<sub>2</sub> (701.23) found ESI-MS, *m/z*: 702.2 (M+H<sup>+</sup>).

**Table 1** Parameters used in HPLC analysis of the prion segments 2a–2g, 3a–3g and 4a–4h

Flow 1 mL/min of ACN in 0.05 % aqueous TFA  
<sup>a</sup> For gradients (Gr) 1–5 an HPLC column Eclipse XDB-C18, 5 μm, 4.6 × 150 mm and for gradients 6–9 an HPLC column Poroshell 120 SB-C18, 2.7 μm, 3 × 50 mm (Agilent Technologies, Santa Clara, CA, USA) were used

Code	ACN concentration (%)	Time (min)	Temperature (°C)	Retention time (min)
Gr <sup>a</sup> 1	0-0-3-58-100	0-2.5-15-26-30	40	10.6(2a), 11.4(2b) 22.9(3a), 25.2(4a)
Gr 2	3-40-100	0-30-40	40	7.0(2c), 6.4(3c)
Gr 3	5-5-26-100	0-2-10-20	27	9.2(2d), 9.3(2e)
Gr 4	5-100	0-40	40	28.4(2f)
Gr 5	12-35-100	0-20-30	40	16.0(3d), 15.0(3e) 20.2(4d), 19.1(4e)
Gr 6	1-1-13-19-57-100	0-1-2-8-13-15	40	7.8(3g), 11.4(4h)
Gr 7	15-33-100	0-6-10	40	3.0(3b), 4.1(4b)
Gr 8	15-60-100	0-25-26	40	16.2, 16.7(3f), 18.8(4f)
Gr 9	15-76-100	0-34-40	40	10.3(2 g), 11.3(4g)

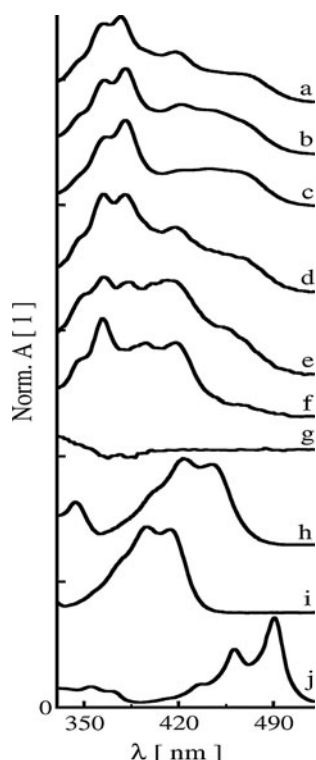


**Fig. 2** Normalized UV-vis spectra of standards, acridinylated rPrP and prion-derived peptides: *a* 9-benzylsulfanyl-6-chloro-2-methoxyacridine (**5**,  $C_{\text{aromatic}}\text{-S}$  bond); *b* H-His-Asp-Cys(Qui)-Val-Asn-OH (**3b**,  $C_{\text{aromatic}}\text{-S}$  bond); *c* H-Glu-Gln-Met-Cys(Qui)-Val-Thr-Asn-OH (**3e**,  $C_{\text{aromatic}}\text{-S}$  bond); *d* [Cys<sup>178</sup>(Qui)]MoPrP178-213 or [Cys<sup>213</sup>(Qui)]MoPrP178-213 (**3f**), 2  $C_{\text{aromatic}}\text{-S}$  bonds; *e* [Cys<sup>178,213</sup>(Qui)]MoPrP178-213 (**4f**), 2  $C_{\text{aromatic}}\text{-S}$  bonds; *f* HisTag-[Cys<sup>178,213</sup>(Qui)]MoPrP23-230 (**4g**), 2  $C_{\text{aromatic}}\text{-S}$  bonds; *g* standard non-acridinylated rPrP (**2g**, no bond to the acridine cycle); *h* quinacrine (**1**,  $C_{\text{aromatic}}\text{-NH}$  bond); *i* 6-chloro-2-methoxy-9-acridone ( $C_{\text{aromatic}}\text{=O}$  bond) and *j* 6-chloro-2-methoxy-9-thioacridone ( $C_{\text{aromatic}}\text{=S}$  bond). The spectrum *g* was normalized to have the same signal amplitude as spectrum (*d*) at 280 nm. Other spectra were normalized to have the maximum in the displayed region

[Asn<sup>217</sup>]HuPrP211-217—H-Glu-Gln-Met-Cys-Ile-Thr-Asn-OH (**2d**)—HPLC RT (Gr 3) 9.1 min. For C<sub>32</sub>H<sub>55</sub>N<sub>9</sub>O<sub>13</sub>S<sub>2</sub> (837.34) found ESI-MS,  $m/z$ : 838.5 (M+H<sup>+</sup>).

[Asn<sup>216</sup>]MoPrP210-216—H-Glu-Gln-Met-Cys-Val-Thr-Asn-OH (**2e**)—HPLC RT (Gr 3) 9.3 min. For C<sub>31</sub>H<sub>53</sub>N<sub>9</sub>O<sub>13</sub>S<sub>2</sub> (823.32) found ESI-MS,  $m/z$ : 824.3 (M+H<sup>+</sup>).

### Method B

Peptide **2f** was synthesized with an automated synthesizer using the FastMoc 0.1 mmol program (SynthAssist<sup>TM</sup> version 3.1) with a single coupling: a 10 eq excess of the protected amino acids and the HBTU coupling reagent and a 20 eq excess of DIPEA were used.

Obtained peptide:

**MoPrP178-213**—H-Cys-Val-Asn-Ile-Thr-Ile-Lys-Gln-His-Thr-Val-Thr-Thr-Thr-Thr-Lys-Gly-Glu-Asn-Phe-Thr-

Glu-Thr-Asp-Val-Lys-Met-Met-Glu-Arg-Val-Val-Glu-Gln-Met-Cys-OH (**2f**)—HPLC RT (Gr 4) 28.4 min. For C<sub>173</sub>H<sub>290</sub>N<sub>48</sub>O<sub>59</sub>S<sub>5</sub> (4,143.98) found ESI-MS,  $m/z$ : 4,145.0 (M+H<sup>+</sup>).

### Recombinant protein synthesis of HisTag-MoPrP23-230 (**2g**)

The gene for the full-length mouse prion protein 23–230 was cloned into the pET-15b expression vector, which contains a sequence for HisTag. After transformation, *E. coli* BL21 (DE3) (Stratagene, La Jolla, CA, USA) was cultivated in Luria broth medium containing ampicillin (100 μg/ml). Recombinant protein expression was induced with 1 mM isopropyl β-D-galactopyranoside. The cells were harvested, resuspended in PBS containing 1 mM PMSF, sonicated, and the cell lysate was treated with DNAase II (5 μg/mL final concentration) to cleave bacterial DNA. The inclusion bodies were twice resuspended in PBS containing 25 % sucrose and 1 % Triton and centrifuged to wash away the membranes and finally solubilized in 50 mM phosphate buffer at pH 8.0 containing 8 M urea and 5 mM β-mercaptoethanol as the reducing agent (Pavliček et al. 2007).

The recombinant prion protein His Tag-MoPrP23-230 (**2g**) (for the full amino acid sequence, see Supporting Information-1) was first purified by affinity chromatography with Ni<sup>2+</sup> resin (Qiagen, Hilden, Germany) under denaturing conditions and then by RP-HPLC with an acetonitrile (ACN) gradient. The purity of the protein was analyzed by MS, SDS-PAGE and UV spectrophotometry. The HPLC RT (Gr 9) was 10.3 min. For C<sub>1093</sub>H<sub>1616</sub>N<sub>344</sub>O<sub>325</sub>S<sub>10</sub> (mono isotopic 25,079; average 25,095) found ESI-MS,  $m/z$ : 25,095 (M<sup>+</sup>), 25,115 (M+Na<sup>+</sup>) (for the more data on MS, see Supporting Information-4).

### General procedure for acridinylation

The thiol containing compound (including glutathione **2h**) and quinacrine dihydrochloride were dissolved in 0.1 M phosphate buffer (pH 7.4–8.0). The solution was kept under argon at 37 °C until the starting material disappeared, which was monitored by HPLC.

### Acridinylated compounds **3a–3h**, **4a–4h**

[Cys(Qui)<sup>178</sup>]MoPrP177-180—H-Asp-Cys(Qui)-Val-Asn-OH (**3a**)—HPLC RT (Gr 1) 22.9 min. <sup>1</sup>H NMR (500 MHz, DMSO) δ 8.90 (d,  $J$  = 8.1 Hz, 1H), 8.70 (d,  $J$  = 9.3 Hz, 1H), 8.21 (dd,  $J$  = 2.2, 0.5 Hz, 1H), 8.30–8.13 (m, 4H), 8.12 (d,  $J$  = 9.4 Hz, 1H), 8.02 (d,  $J$  = 8.9 Hz, 1H), 7.89 (d,  $J$  = 2.7 Hz, 1H), 7.72 (dd,  $J$  = 9.3, 2.2 Hz, 1H), 7.62 (dd,  $J$  = 9.4, 2.8 Hz, 1H), 7.38 (s, 1H), 6.88 (s, 1H), 4.57

(td,  $J = 8.3, 6.0$  Hz, 1H), 4.50 (ddd,  $J = 7.7, 6.9, 5.8$  Hz, 1H), 4.19 (dd,  $J = 8.9, 6.3$  Hz, 1H), 4.06 (m, 1H), 4.04 (s, 3H), 3.35 (dd,  $J = 12.8, 5.7$  Hz, 1H), 3.11 (dd,  $J = 12.8, 8.6$  Hz, 1H), 2.82 (dd,  $J = 17.9, 3.4$  Hz, 1H), 2.65 (dd,  $J = 18.0, 8.9$  Hz, 1H), 2.54 (dd,  $J = 15.7, 5.8$  Hz, 1H), 2.45 (dd,  $J = 15.7, 6.9$  Hz, 1H), 1.95 (septet of d,  $J = 6.8, 6.3$  Hz, 1H), 0.82 (d,  $J = 6.8$  Hz, 3H), 0.78 (d,  $J = 6.8$  Hz, 3H).  $^{13}\text{C}$  NMR (126 MHz, DMSO)  $\delta$  172.67, 171.10, 170.91, 170.19, 168.66, 167.93, 158.20, 146.40, 145.99, 139.28, 134.09, 131.75, 129.65, 128.60, 128.07, 127.87, 127.29, 126.14, 102.23, 57.41, 55.89, 53.28, 48.86, 48.69, 38.18, 36.49, 35.46, 30.90, 19.08, 17.80 (for the structure of the molecule, see Supporting Information-2). For  $\text{C}_{30}\text{H}_{35}\text{N}_6\text{O}_9\text{SCl}$  (690.19) found ESI-MS,  $m/z$ : 691.2 ( $\text{M}+\text{H}^+$ ).

**[Cys(Qui) $^{178}$ ]MoPrP176-180**—H-His-Asp-Cys(Qui)-Val-Asn-OH (**3b**)—During the reaction, the yellow product started to precipitate as a gel. The reaction mixture was cooled to 0 °C to support precipitation. The precipitate was separated by centrifugation and washed several times with water until the supernatant was colorless. The precipitate was dissolved in a minimal amount of 50 % AcOH and purified by HPLC with a yield of 80 %. HPLC RT (Gr 7) 3.0 min.  $^1\text{H}$  NMR (600 MHz, DMSO)  $\delta$  8.92 (s, 1H), 8.87 (d,  $J = 6.8$  Hz, 1H), 8.82 (d,  $J = 6.0$  Hz, 1H), 8.74 (d,  $J = 9.3$  Hz, 1H), 8.22 (d,  $J = 7.6$  Hz, 1H), 8.20 (d,  $J = 2.1$  Hz, 1H), 8.11 (d,  $J = 9.4$  Hz, 1H), 7.91 (d,  $J = 2.8$  Hz, 1H), 7.79 (d,  $J = 9.0$  Hz, 1H), 7.68 (dd,  $J = 9.3, 2.2$  Hz, 1H), 7.61 (dd,  $J = 9.4, 2.8$  Hz, 1H), 7.47 (s, 1H), 7.39 (d,  $J = 1.3$  Hz, 1H), 6.90 (d,  $J = 1.3$  Hz, 1H), 4.66–4.60 (m, 1H), 4.50–4.44 (m, 2H), 4.17 (dd,  $J = 9.0, 6.2$  Hz, 1H), 4.15 (t,  $J = 6.3$  Hz, 1H), 4.02 (s, 3H), 3.36 (dd,  $J = 13.0, 4.9$  Hz, 1H), 3.25–3.17 (m, 2H), 3.14 (dd,  $J = 13.0, 10.2$  Hz, 1H), 2.77 (dd,  $J = 17.2, 3.6$  Hz, 1H), 2.55 (dd,  $J = 17.2, 9.5$  Hz, 1H), 2.53–2.51 (m, 1H), 2.43 (dd,  $J = 15.8, 7.1$  Hz, 1H), 1.92 (septet of d,  $J = 6.8, 6.2$  Hz, 1H), 0.80 (d,  $J = 6.8$  Hz, 3H), 0.75 (d,  $J = 6.8$  Hz, 3H).  $^{13}\text{C}$  NMR (150 MHz, DMSO)  $\delta$  172.78, 171.33, 171.19, 171.16, 170.35, 169.00, 167.49, 158.28, 146.47, 146.05, 139.51, 134.59, 134.20, 131.79, 129.84, 128.78, 128.15, 127.92, 127.42, 126.85, 126.32, 118.26, 102.30, 57.23, 55.95, 53.46, 51.24, 50.07, 48.75, 38.23, 36.51, 36.06, 31.12, 26.76, 19.15, 17.79 (for the structure of the molecule, see Supporting Information-2). For  $\text{C}_{36}\text{H}_{42}\text{N}_9\text{O}_{10}\text{SCl}$  (828.31) found ESI-MS,  $m/z$ : 829.3 ( $\text{M}+\text{H}^+$ ).

**[Thz $^{175}$ ,Cys (Qui) $^{178}$ ]MoPrP175-180**—H-Thz-His-Asp-Cys(Qui)-Val-Asn-OH (**3c**)—HPLC RT (Gr 2) 6.4 min. For  $\text{C}_{40}\text{H}_{47}\text{N}_{10}\text{O}_{11}\text{S}_2\text{Cl}$  (942.26) found ESI-MS,  $m/z$ : 943.3 ( $\text{M}+\text{H}^+$ ).

**[Cys(Qui) $^{179}$ ,Asn $^{217}$ ]HuPrP211-217**—H-Glu-Gln-Met-Cys(Qui)-Ile-Thr-Asn-OH (**3d**)—HPLC RT (Gr 5) 16.0 min. For  $\text{C}_{46}\text{H}_{63}\text{N}_{10}\text{O}_{14}\text{S}_2\text{Cl}$  (1078.37) found ESI-MS,  $m/z$ : 1,079.4 ( $\text{M}+\text{H}^+$ ).

**[Cys(Qui) $^{213}$ ,Asn $^{216}$ ]MoPrP210-216**—H-Glu-Gln-Met-Cys(Qui)-Val-Thr-Asn-OH (**3e**)—HPLC RT (Gr 5) 15.0 min.  $^1\text{H}$  NMR (500 MHz, DMSO)  $\delta$  8.70 (d,  $J = 9.4$  Hz, 1H), 8.65 (d,  $J = 7.5$  Hz, 1H), 8.47 (d,  $J = 8.0$  Hz, 1H), 8.24 (d,  $J = 8.0$  Hz, 1H), 8.20 (dd,  $J = 2.2, 0.4$  Hz, 1H), 8.14 (d,  $J = 4.1$  Hz, 3H), 8.11 (d,  $J = 9.4$  Hz, 1H), 7.97 (d,  $J = 8.7$  Hz, 1H), 7.92 (d,  $J = 8.2$  Hz, 1H), 7.90 (d,  $J = 2.8$  Hz, 1H), 7.80 (d,  $J = 8.4$  Hz, 1H), 7.68 (dd,  $J = 9.3, 2.2$  Hz, 1H), 7.60 (dd,  $J = 9.4, 2.8$  Hz, 1H), 7.37 (s, 1H), 7.26 (s, 1H), 6.89 (s, 1H), 6.81 (s, 1H), 4.53–4.44 (m, 2H), 4.39–4.31 (m, 2H), 4.22 (dd,  $J = 8.7, 6.8$  Hz, 1H), 4.19 (dd,  $J = 8.5, 4.1$  Hz, 1H), 4.01 (s, 3H), 3.90 (qd,  $J = 6.4, 4.1$  Hz, 1H), 3.86–3.81 (m, 1H), 3.28 (dd,  $J = 12.9, 4.9$  Hz, 1H), 3.17 (dd,  $J = 12.9, 9.6$  Hz, 1H), 2.50 (2H, overlapped by the solvent peak; chemical shift was determined from the HSQC and HMBC data), 2.47–2.33 (m, 4H), 2.24–2.09 (m, 2H), 2.00 (s, 3H), 1.98–1.70 (m, 7H), 0.97 (d,  $J = 6.4$  Hz, 3H), 0.80 (d,  $J = 6.8$  Hz, 3H), 0.76 (d,  $J = 6.8$  Hz, 3H).  $^{13}\text{C}$  NMR (126 MHz, DMSO)  $\delta$  173.62, 173.41, 172.52, 171.33, 171.19, 170.70, 170.57, 169.40, 169.38, 168.07, 158.13, 146.41, 145.97, 139.34, 134.04, 131.66, 129.80, 128.61, 127.99, 127.83, 127.30, 126.18, 102.14, 66.57, 57.75, 57.69, 55.78, 53.08, 52.43, 51.83, 51.44, 48.49, 38.28, 36.62, 32.31, 31.49, 30.52, 29.29, 28.96, 27.84, 26.53, 19.21, 19.12, 17.91, 14.6 (for the structure of the molecule, see Supporting Information-2). For  $\text{C}_{45}\text{H}_{61}\text{N}_{10}\text{O}_{14}\text{S}_2\text{Cl}$  (1,064.4) found ESI-MS,  $m/z$ : 1,065.3 ( $\text{M}+\text{H}^+$ ).

**[Cys(R) $^{178,213}$ ]MoPrP178-213**—mono-acridinylated derivative: H-Cys(R)-Val-Asn-Ile-Thr-Ile-Lys-Gln-His-Thr-Val-Thr-Thr-Thr-Thr-Lys-Gly-Glu-Asn-Phe-Thr-Glu-Thr-Asp-Val-Lys-Met-Met-Glu-Arg-Val-Val-Glu-Gln-Met-Cys(R)-OH (**3f**), **R** = Qui and/or H. Prior to analytical HPLC, 40  $\mu\text{L}$  of the sample was diluted with ACN (20  $\mu\text{L}$ ), AcOH (55  $\mu\text{L}$ ),  $(\text{CF}_3)_2\text{CH-OH}$  (10  $\mu\text{L}$ ) and TFA (25  $\mu\text{L}$ ). HPLC RT (Gr 8) was 16.2 and 16.7 min, respectively. For  $\text{C}_{187}\text{H}_{298}\text{N}_{49}\text{O}_6\text{S}_5\text{Cl}$  (4,385.21) found ESI-MS,  $m/z$ : 4,386.3 ( $\text{M}+\text{H}^+$ ).

**S-(6-chloro-2-methoxyacridin-9-yl)glutathione (3g)**—HPLC RT (Gr 6) 7.8 min.  $^1\text{H}$  NMR (400 MHz, DMSO)  $\delta$  8.66 (d,  $J = 9.2$  Hz, 1H), 8.42 (d,  $J = 8.3$  Hz, 1H), 8.31–8.23 (m, 4H), 8.22 (d,  $J = 2.1$  Hz, 1H), 8.11 (d,  $J = 9.4$  Hz, 1H), 7.89 (d,  $J = 2.7$  Hz, 1H), 7.69 (dd,  $J = 9.3, 2.1$  Hz, 1H), 7.61 (dd,  $J = 9.4, 2.7$  Hz, 1H), 4.39 (ddd,  $J = 9.4, 8.3, 4.7$  Hz, 1H), 4.02 (s, 3H), 3.92–3.85 (m, 1H), 3.58 (d,  $J = 5.9$  Hz, 2H), 3.33 (dd,  $J = 13.3, 4.7$  Hz, 1H), 3.18 (dd,  $J = 13.3, 9.4$  Hz, 1H), 2.28–2.14 (m, 2H), 2.00–1.86 (m, 2H).  $^{13}\text{C}$  NMR (151 MHz, DMSO)  $\delta$  171.03, 170.85, 170.79, 169.88, 158.10, 146.44, 145.93, 139.38, 134.00, 131.66, 129.90, 128.52, 128.00, 127.83, 127.14, 126.19, 102.28, 55.71, 53.03, 51.67, 40.62, 38.59,

30.65, 25.84 (for the structure of the molecule, see Supporting Information-2). For  $C_{24}H_{25}N_4O_7SCl$  (548.11) found ESI-MS,  $m/z$ : 549.1 ( $M+H^+$ ).

**Qui-[Cys(Qui)<sup>178</sup>]MoPrP177-180**—Qui-Asp-Cys(Qui)-Val-Asn-OH (**4a**)—HPLC RT (Gr 1) 25.2 min. For  $C_{44}H_{43}N_7O_{10}SCl_2$  (931.22) found ESI-MS,  $m/z$ : 932.2 ( $M+H^+$ ).

**Qui-[Cys(Qui)<sup>178</sup>]MoPrP175-180**—Qui-His-Asp-Cys(Qui)-Val-Asn-OH (**4b**)—10 % yield, HPLC RT (Gr 7) 4.1 min. For  $C_{50}H_{50}N_{10}O_{11}SCl_2$  (1,068.28) found ESI-MS,  $m/z$ : 1,069.3 ( $M+H^+$ ).

**[Thz<sup>175</sup>,Cys (Qui)<sup>178</sup>]MoPrP175-180**—H-Thz-His(Qui)-Asp-Cys(Qui)-Val-Asn-OH (**4c**)—HPLC RT (Gr 7). This compound was not detected because the imidazole nucleus of the His residue was not modified with quinacrine.

**Qui-[Cys(Qui)<sup>214</sup>,Asn<sup>217</sup>]HuPrP211-217**—Qui-Glu-Gln-Met-Cys(Qui)-Ile-Thr-Asn-OH (**4d**)—HPLC RT (Gr 5) 20.2 min. For  $C_{60}H_{71}N_{11}O_{15}S_2Cl_2$  (1,319.39) found ESI-MS,  $m/z$ : 1,320.4 ( $M+H^+$ ).

**Qui-[Cys(Qui)<sup>213</sup>,Asn<sup>216</sup>]MoPrP210-216**—Qui-Glu-Gln-Met-Cys(Qui)-Val-Thr-Asn-OH (**4e**)—HPLC RT (Gr 5) 19.1 min. For  $C_{59}H_{69}N_{11}O_{15}S_2Cl_2$  (1,305.31) found ESI-MS,  $m/z$ : 1,305.9 ( $M+H^+$ ).

**[Cys(Qui)<sup>178,213</sup>]MoPrP178-213**—H-Cys(Qui)-Val-Asn-Ile-Thr-Ile-Lys-Gln-His-Thr-Val-Thr-Thr-Thr-Lys-Gly-Glu-Asn-Phe-Thr-Glu-Thr-Asp-Val-Lys-Met-Met-Glu-Arg-Val-Val-Glu-Gln-Met-Cys(Qui)-OH (**4f**). Prior to HPLC analysis, 30  $\mu$ L of the sample was diluted with ACN (15  $\mu$ L), AcOH (40  $\mu$ L),  $(CF_3)_2CH-OH$  (10  $\mu$ L) and TFA (20  $\mu$ L). HPLC RT (Gr 8) was 18.8 min. For  $C_{201}H_{306}N_{50}O_{61}S_5Cl_2$  (4,626.04) found ESI-MS,  $m/z$ : 4,627.1 ( $M+H^+$ ).

**HisTag-[Cys(Qui)<sup>178,213</sup>]MoPrP23-230 (4g)** (for the full amino acid sequence, see Supporting Information-1). Prion protein **2g** (5.03 mg) and quinacrine dihydrochloride (15.44 mg) were dissolved in a solution of 6 M guanidine hydrochloride in 0.1 M phosphate buffer (1.0 mL) and ACN (0.3 mL). After the reaction was finished, the crude reaction mixture was pre-purified by gel filtration on Sephadex G10. Only a bis-acridinylated product was detected. HPLC RT (Gr 9) 11.3 min. For  $C_{1121}H_{1632}N_{346}O_{327}S_{10}Cl_2$  (mono isotopic 2,5562; average 25,579) found ESI-MS,  $m/z$ : 25,579 ( $M^+$ ), 25,610 ( $M+K^+$ ) (for the more data on MS, see Supporting Information-4).

**N,S-bis(6-chloro-2-methoxyacridin-9-yl)glutathione (4h)**—HPLC RT (Gr 6) 11.4 min. For  $C_{38}H_{33}N_5O_8SCl_2$  (789.14) found ESI-MS,  $m/z$ : 790.1 ( $M+H^+$ ).

**9-Benzylsulfanyl-6-chloro-2-methoxyacridine (5)**—The compound was prepared according to our published procedure (Zawada et al. 2011) and was obtained as an orange solid; m.p. 153–155 °C. <sup>1</sup>H-NMR (400 MHz,

$CDCl_3$ )  $\delta$  8.47 (dd,  $J = 9.3, 0.4$  Hz, 1H), 8.10 (dd,  $J = 2.1, 0.4$  Hz, 1H), 7.98 (dd,  $J = 9.4, 0.4$  Hz, 1H), 7.66 (dd,  $J = 2.8, 0.4$  Hz, 1H), 7.36 (m, 2H), 7.05–6.93 (m, 3H), 6.78 (m, 2H), 3.94 (s, 2H), 3.83 (s, 3H). <sup>13</sup>C NMR (101 MHz,  $CDCl_3$ )  $\delta$  158.3, 147.1, 146.6, 139.0, 137.4, 135.0, 131.7, 130.8, 128.8, 128.5, 128.5, 128.0, 127.9, 127.5, 126.1, 102.3, 55.7, 41.4. HRMS (EI) calculated for  $C_{21}H_{16}NOSCl$  365.0641, found 365.0643.

#### *Incubation of oxidized and reduced HuPrP23-230 with quinacrine*

The oxidized **HuPrP23-230** (Alicon, 1 mg/mL) was diluted to a final concentration of 0.25 mg/mL in a 50 mM phosphate buffer at pH 8.3 containing 50, 10 or 0  $\mu$ M of quinacrine and was incubated for 4 days at 37 °C. Aliquots were taken every 24 h, immediately frozen on dry ice and stored at –80 °C.

The oxidized **HuPrP23-230** (Alicon, 1 mg/mL) and BSA were diluted to final concentrations of 0.25 mg/mL in phosphate-buffered saline at pH 7.4. The reduced samples were prepared by a 24 h incubation of the oxidized samples with 5 mM  $\beta$ -mercaptoethanol at 4 °C. All of the samples were then incubated in the presence of 10 or 0  $\mu$ M quinacrine for 2.5 days at 37 °C.

The samples were loaded onto a 12 % SDS-PAGE gel containing glycerol and separated by electrophoresis (90 min, 100 V). The gel was transilluminated by UV light (an orange filter KENKO SO-56 55 mm YA3) with a 15 s exposure and then stained with Coomassie brilliant blue.

#### *Trypsin cleavage*

In order to lower trypsin efficiency to obtain longer fragments of trypsin cleavage, we used Milli-Q water instead of buffer when preparing corresponding solutions. A buffer usage has led to complicated mixtures of short fragments.

Unlabeled (**2g**) and labeled (**4g**) prion proteins were cleaved with trypsin: 1  $\mu$ L of peptide solution (2  $\mu$ g/ $\mu$ L), and 0.5  $\mu$ L of trypsin solution (1  $\mu$ g/ $\mu$ L) were added to 18.5  $\mu$ L of water, and the reaction mixtures were stirred at 38 °C for 8 h. The cleaved fragments were then analyzed by mass spectrometry. From many fragments we show only the fragments (**6a–6e**) with Qui label (for MALDI-MS fingerprints, see Supporting Information-3).

Identified fragments present in only the labeled protein **[Cys(Qui)<sup>178</sup>]MoPrP156-193 (6a)**—H-Tyr-Pro-Asn-Gln-Val-Tyr-Tyr-Arg-Pro-Val-Asp-Gln-Tyr-Ser-Asn-Gln-Asn-Asn-Phe-Val-His-Asp-Cys(Qui)-Val-Asn-Ile-Thr-Ile-Lys-Gln-His-Thr-Val-Thr-Thr-Thr-Lys-OH—For  $C_{214}H_{310}N_{57}O_{64}SCl$  (monoisotopic 4,769.22; avg 4,772.62) found MALDI-MS,  $m/z$ : 4,772.6 ( $M^+$ ).

**Table 2** The acridinylation efficiency for cysteine thiol group in various peptides

Item	Source of thiol group	S-acridinylated	N,S-bisacridinylated	Reaction time (h)
1	MoPrP177-180 <sup>a</sup> ( <b>2a</b> )	100 % ( <b>3a</b> )	Traces ( <b>4a</b> )	18
2	MoPrP176-180 ( <b>2b</b> )	80 % <sup>c,d</sup> ( <b>3b</b> )	10 % <sup>c,d</sup> ( <b>4b</b> )	17
3	MoPrP176-180 <sup>a</sup> ( <b>2b</b> )	90 % <sup>e</sup> ( <b>3b</b> )	10 % <sup>e</sup> ( <b>4b</b> )	17
4	MoPrP176-180 <sup>b</sup> ( <b>2b</b> )	35 % <sup>e</sup> ( <b>3b</b> )	65 % <sup>e</sup> ( <b>4b</b> )	17
5	[Thz <sup>175</sup> ]MoPrP175-180 <sup>a</sup> ( <b>2c</b> )	100 % <sup>d</sup> ( <b>3c</b> )	0 % <sup>e</sup>	14
6	[Asn <sup>217</sup> ]HuPrP211-217 ( <b>2d</b> )	100 % <sup>e</sup> ( <b>3d</b> )	Traces <sup>e</sup> ( <b>4d</b> )	24
7	[Asn <sup>216</sup> ]MoPrP210-216 ( <b>2e</b> )	100 % <sup>e</sup> ( <b>3e</b> )	Traces <sup>e</sup> ( <b>4e</b> )	24
8	Reduced glutathione	95 % <sup>e</sup> ( <b>3h</b> )	Traces <sup>e</sup> ( <b>4h</b> )	48
9	Oxidized glutathione	0 % <sup>e</sup>	0 % <sup>f</sup>	216
10	Bzl-SH	98 % <sup>e</sup> ( <b>5</b> )	–	23

Reactions were performed under argon at pH 7.4–8.0, 37 °C and a ratio peptide versus quinacrine 1:4

<sup>b</sup> In solution

<sup>c</sup> In gel

<sup>d</sup> Entire reaction mixture (total solution + gel)

<sup>e</sup> Preparative yield

<sup>f</sup> HPLC yield

[Cys(Qui)<sup>178</sup>]MoPrP156-203 (**6b**)—H-Tyr-Pro-Asn-Gln-Val-Tyr-Tyr-Arg-Pro-Val-Asp-Gln-Tyr-Ser-Asn-Gln-Asn-Asn-Phe-Val-His-Asp-Cys(Qui)-Val-Asn-Ile-Thr-Ile-Lys-Gln-His-Thr-Val-Thr-Thr-Thr-Lys-Gly-Glu-Asn-Phe-Thr-Glu-Thr-Asp-Val-Lys-OH—For C<sub>262</sub>H<sub>382</sub>N<sub>69</sub>O<sub>83</sub>S<sub>1</sub>Cl (monoisotopic 5,889.72; avg 5,893.78) found MALDI-MS, *m/z*: 5,893.3 (M<sup>+</sup>).

[Cys(Qui)<sup>178</sup>]MoPrP151-203 (**6c**)—H-Glu-Asn-Met-Tyr-Arg-Tyr-Pro-Asn-Gln-Val-Tyr-Tyr-Arg-Pro-Val-Asp-Gln-Tyr-Ser-Asn-Gln-Asn-Asn-Phe-Val-His-Asp-Cys(Qui)-Val-Asn-Ile-Thr-Ile-Lys-Gln-His-Thr-Val-Thr-Thr-Thr-Lys-Gly-Glu-Asn-Phe-Thr-Glu-Thr-Asp-Val-Lys-OH—For C<sub>291</sub>H<sub>425</sub>N<sub>78</sub>O<sub>92</sub>S<sub>2</sub>Cl (monoisotopic 6,583.01; avg 6,587.55) found MALDI-MS, *m/z*: 6,588.4 (M+H<sup>+</sup>).

[Cys(Qui)<sup>178,213</sup>]MoPrP156-219 (**6d**)—H-Tyr-Pro-Asn-Gln-Val-Tyr-Tyr-Arg-Pro-Val-Asp-Gln-Tyr-Ser-Asn-Gln-Asn-Asn-Phe-Val-His-Asp-Cys(Qui)-Val-Asn-Ile-Thr-Ile-Lys-Gln-His-Thr-Val-Thr-Thr-Thr-Thr-Lys-Gly-Glu-Asn-Phe-Thr-Glu-Thr-Asp-Val-Lys-Met-Met-Glu-Arg-Val-Val-Glu-Gln-Met-Cys(Qui)-Val-Thr-Gln-Tyr-Gln-Lys-OH—For C<sub>359</sub>H<sub>527</sub>N<sub>93</sub>O<sub>109</sub>S<sub>5</sub>Cl<sub>2</sub> (monoisotopic 8,114.65; avg 8,120.84) found MALDI-MS, *m/z*: 8,119.3.

[Cys(Qui)<sup>178,213</sup>]MoPrP156-228 (**6e**)—H-Tyr-Pro-Asn-Gln-Val-Tyr-Tyr-Arg-Pro-Val-Asp-Gln-Tyr-Ser-Asn-Gln-Asn-Asn-Phe-Val-His-Asp-Cys(Qui)-Val-Asn-Ile-Thr-Ile-Lys-Gln-His-Thr-Val-Thr-Thr-Thr-Thr-Lys-Gly-Glu-Asn-Phe-Thr-Glu-Thr-Asp-Val-Lys-Met-Met-Glu-Arg-Val-Val-Glu-Gln-Met-Cys(Qui)-Val-Thr-Gln-Tyr-Gln-Lys-Glu-Ser-Gln-Ala-Tyr-Tyr-Asp-Gly-Arg-OH—For C<sub>405</sub>H<sub>590</sub>N<sub>106</sub>O<sub>126</sub>S<sub>5</sub>Cl<sub>2</sub> (monoisotopic 9,184.10; avg 9,190.91) found MALDI-MS, *m/z*: 9,190.7 (M<sup>+</sup>).

## Results and discussion

Reactions of small prion-derived peptides provided products that could be characterized by common analytical methods (Table 2; Fig. 1). The PrP<sup>C</sup> contains only two Cys residues forming a disulfide bridge. The model peptides were chosen based on symmetry because the Cys residue is located in the middle of their sequences. Cys ± 2 amino acids in the H-His-Asp-Cys-Val-Asn-OH (**2b**) denote both mouse (Mo)PrP176-180 and human (Hu)PrP177-181, and Cys ± 3 amino acids in the H-Glu-Gln-Met-Cys-Val-Thr-Asn-OH (**2e**) and H-Glu-Gln-Met-Cys-Ile-Thr-Asn-OH (**2d**) correspond to [Asn<sup>216</sup>]MoPrP210-216 and [Asn<sup>217</sup>]HuPrP211-217, respectively. The Q216N or Q217N mutations at the Cys + 3 position simplified the synthesis of a small peptide series because the same starting resin loaded with Fmoc-Asn(Trt)-OH could be used for several peptides. The mutated peptide was shortened by one methylene group, presumably without a significant effect on the peptide secondary structure and reactivity.

### Reactivity of prion cysteines with quinacrine

The most detailed study was conducted with MoPrP176-180 (**2b**), which could serve as an equivalent for HuPrP177-181. During the reaction with quinacrine, this peptide formed a gel, which is an intrinsic property of some prion-derived peptides and especially of PrP<sup>C</sup> (Wille et al. 2009; Ronga et al. 2007). The gel formation complicated the establishment of a kinetic assay for the exchange of the amino substituent for a sulfide substituent. According to an

HPLC analysis of the gel and corresponding solution, a higher solubility was observed for H-His-Asp-Cys(Qui)-Val-Asn-OH (**3b**) in comparison to the bis-acridinylated compound, Qui-His-Asp-Cys(Qui)-Val-Asn-OH (**4b**) (Table 2, items 3 and 4). **3b** was obtained as the main product, whereas the minor by-product, **4b**, was separable by centrifugation. The sites of acridinylation were confirmed by NMR spectroscopy and MS spectrometry. An investigation of MoPrP176-180 (**3b**) confirmed that Cys<sup>178</sup> is prone to acridinylation at the sulfur atom.

The asparagine mutants MoPrP210-216 (**2e**) and HuPrP211-217(**2d**) containing Cys<sup>213</sup> and Cys<sup>214</sup> also reacted with quinacrine. For these peptides, only traces of the bis-acridinylated peptides were obtained (Table 2, items 6 and 7). Thus, both Cys residues of MoPrP and HuPrP also have the potential to capture an aromatic acridine ring via their nucleophilic thiol groups.

In contrast to the previously observed chemical reactivity of glutathione (Wild and Young 1965), our analysis, which was empowered by preparative RP-HPLC, indicated that the main product was the mono-*S*-acridinylated compound (**3g**). The mono-acridinylated species were observed in all of our experiments as the main products, whereas Wild and Young (1965) could neither isolate them, nor observe them by TLC.

The *N,S*-bis-acridinylated compound (**4b**) was only formed in a sufficient amount after 17 h of reaction time if an N-terminal His residue was present. In the absence of an N-terminal His, a similar peptide sequence only provided compound **4a**, as a trace impurity (Table 2, item 1). Therefore, we deduced that the N-terminal His residue accelerates the formation of the *N,S*-bis-acridinylated species. To determine whether acridinylation occurred on the imidazole ring or on the N-terminal amino group of His, we blocked the N-terminal amino group with 4-thiazolidine carboxylic acid (Thz, **2c**). This amino acid contains a secondary amino group, which is not prone to acridinylation by an acridine transfer reaction (Šebestík et al. 2006). As expected, only the corresponding compound **3c** with Cys(Qui) was formed; we did not detect a compound containing a His(Qui) residue (Table 2, Item 5). Formation of a stable *N*-acridinylated imidazole species was thus excluded.

MoPrP178-213 (**2f**) was used to explore the susceptibility of prion cysteines to acridinylation in more complex substrates. This peptide contains both of the Cys residues found in the prion protein. Although the reaction was performed in 6 M guanidine (0.1 M phosphate buffer, pH 8), the peptide and product formed a gel or precipitate. Despite the limited solubility, both mono- and *S,S'*-bis-acridinylated derivatives of MoPrP178-213 (**3f**, **4f**) were detected and identified. The mono-acridinylated product, **3f**, could be detected and isolated by HPLC. However, **3f**

was only isolated in amounts sufficient for molecular mass estimation (MALDI-TOF) and not for NMR experiments, by which we could have elucidated the site of quinacrine substitution in the peptide. The mono-acridinylated derivative was converted to the bis-acridinylated derivative with a prolonged reaction time (about ~30 h). However, even after 10 days, the amount of the bis-acridinylated product was quite low. This result can be mainly attributed to oxidation of four sulfur atoms in this molecule (Cys and Met residues) with the subsequent formation of many different products. Even if only the sulfide, (*R*)-sulfoxide and (*S*)-sulfoxide are considered, there is the potential for the generation of  $4^3 = 64$  compounds. Indeed, we have observed adducts of the products and a reactant with oxygen atoms by MS analysis.

The recombinant mouse protein HisTag-MoPrP23-230 (**2g**) was chosen as the closest model of native PrP<sup>C</sup> (see recombinant protein synthesis in the “Materials and methods”). This protein was also prone to gel formation, which required a variation in the reaction conditions including the introduction of an organic co-solvent (17 % ACN). The organic co-solvent can be viewed as the simplest model of a biological membrane (it at least has a lower relative permittivity than water), where the native PrP<sup>C</sup> is anchored (Cobb and Surewicz 2009; Franks et al. 1993). In contrast to the previous model peptides, the reactivity of the HisTag-MoPrP23-230 (**2g**) was significantly lower and the reaction times were longer. In this case, oxidation also significantly limited the evaluation of the reaction. The protein contains ten sulfur atoms—including the Met residues—and can form more than 1,000 by-products. In fact, we have observed significant formation of oxidized derivatives of this molecule. The decreased reactivity of this protein can be attributed to several factors such as its lower solubility, higher molecular mass (Yamamoto and Miller 2005), lower stability and conformational pre-organization for disulfide bridge formation (Tompa et al. 2002; Lehn 1993). Despite the protein decomposition, we were successful in the preparation of the bis-acridinylated derivative **4g**.

According to HPLC, MS and NMR analyses of compounds **3a–3e**, the reactivity of amino acids including Asp, Asn, Cys, Glu, His, Met, Gln, Thr and Thz with quinacrine is limited to the thiol group of Cys and, to lesser extent, the N-terminal amino group of His. In contrast to common labeling reagents based on alkylation such as alkyl halides, quinacrine does not react with the Met sulfide group (Flavell et al. 2002). It was previously shown that the reactivity of the amino group is governed by its  $pK_a$  (Paul and Ladame 2009). Thus, under aqueous physiological conditions, Lys and Arg are not susceptible to acridinylation. This fact may explain the bis-acridinylation of MoPrP178-213 (**2f**), which contains two Cys, one Arg, and

three Lys. Tris- and oligo-acridinylations were not observed by LC–MS techniques.

#### UV–vis spectra of acridinylated compounds (Fig. 2)

The attachment of an acridine moiety to a thiol group led to a characteristic absorption spectrum in the visible region (Claude et al. 1989), which was in agreement with our observations (Fig. 2), in which model peptides and labeled benzyl mercaptan afforded similar UV–vis spectra in the 365–381 nm region, followed by a plateau formed by a cluster of peaks ceasing at about 500 nm (vibrationally resolved UV–vis). In some cases, the flatness of the plateau hampered the location of peaks maxima. For example, the acridine residue linked to MoPrP176-180 (**3b**) provided a characteristic absorption pattern with maxima at 365, 381 and 422 nm (Fig. 2b), whereas the maxima observed in the labeled [Asn<sup>216</sup>]MoPrP210-216 (**3e**) were at 366, 381, 425, 438 and 442 nm (Fig. 2c). Similar characteristic absorptions were also observed for the model of the prion peptide containing both Cys residues [Cys(R)<sup>178,213</sup>]MoPrP178-213 (**3f**, R = Qui and/or H, Fig. 2d), with maxima at 364, 381 and 420 nm. The UV–vis spectrum of [Cys(Qui)<sup>178,213</sup>]MoPrP178-213 (**4f**, Fig. 2e) is similar to the spectra of the mono-acridinylated species (**3b**, **3e**, **3f** and **5**; Fig. 2a–d), which indicates that the acridinylation also takes place at the sulfur atoms of thiol groups. A labeling of the HisTag-MoPrP23-230 (**2g**, Fig. 2f) led to the bis-acridinylated species (**4g**), only. It correlates well with the presence of two Cys residues in the prion protein.

The quality of the spectra was significantly affected by a lower effective concentration of the acridine moiety: the mass fraction of acridine is 30 % in MoPrP176-180 (**3b**), 11 % in MoPrP178-213 (**4f**) and 2 % in the protein (**4g**). The quality of the spectra was also affected by the significantly lower solubility of the conjugate. The spectrum of the labeled protein (**4g**, Fig. 2e) is quantitatively similar to the model spectra of the modified MoPrP176-180 (**3b**, Fig. 2b), [Asn<sup>216</sup>]MoPrP210-216 (**3e**, Fig. 2c) and MoPrP178-213 (**3f**, Fig. 2d).

The UV–vis spectra of the S-acridinylated peptides were able to serve as convenient “fingerprints” providing quickly acquired an interpreted information about the product. The product from the quinacrine reaction that contained a C<sub>aromatic</sub>–NH bond (Fig. 2h), and the by-products: 6-chloro-2-methoxy-9-acridone, containing a C<sub>aromatic</sub>=O bond (Lewis 1949); and 6-chloro-2-methoxy-9-thioacridone, containing a C<sub>aromatic</sub>=S bond (Gaydukevich et al. 1987); (Fig. 2i, j), respectively (for both the by-product structures, see Supporting Information-2), could be distinguished from the peptides, containing a C<sub>aromatic</sub>–S bond (Fig. 2b–f) by merely a simple comparison of their UV–vis spectra. When the acridine moiety is

not attached to the peptide sulfur atom but to the sulfur atom of benzyl mercaptan (**5**, Fig. 2a), the characteristic UV–vis pattern is not changed. Thus, we can conclude that the UV–vis spectrum of the acridine moiety is not sensitive toward the identity of the alkyl chain attached to the sulfur atom.

However, the replacement of the sulfur atom at C-9 of acridine by another atom (H, N or O) altered the spectrum significantly. The strong sensitivity of the UV–vis spectrum to the atom directly attached to the C-9 position and the bond order between C-9 and this atom indicated that this method could be used for qualitative analysis of the sample. The ratio of the maximum at 366 nm to the maximum at 381 nm slightly changes with the molecular weight of the C-9 substituent (Fig. 2a–f). The region of the spectrum at about 400–500 nm flattens with increasing molecular weight. In the case of the prion protein (Fig. 2f), the plateau is blue-shifted toward the maximum at 366 nm.

#### Fluorescence spectra of acridinylated compounds (Fig. 3; Table 3)

Fluorescence spectroscopy provides characteristic patterns for various acridine labels, and is more sensitive than UV–vis spectroscopy. For example, labeling of Cys by quinacrine led to a 40 nm blue shift of the emission maximum from that of quinacrine (Fig. 3).

On the basis of the fluorescence spectra, we can also exclude non-covalent binding, which was also described for 9-aminoacridines, PrP<sup>C</sup>, and PrP<sup>Sc</sup> (Phuan et al. 2007; Vogtherr et al. 2003). Comparing the spectra of the labeled protein conjugate **4g** and the quinacrine (**1**)–protein **2g** mixture (2:1) (Fig. 3d, f), it is obvious that the spectrum of the non-covalent mixture (Fig. 3f) resembles the spectrum of unmodified neat quinacrine (Fig. 3e), and that the spectrum of the labeled protein conjugate **4g** (Fig. 3d) is similar to the spectra of the labeled peptides (**3a**, **3b**, **3e**) (Fig. 3a–c). The small difference in wavelength between the labeled protein **4g** and peptides **3a**, **3b**, **3e** (14 nm) can be attributed to the more hydrophobic environment inside the protein. Thus, the fluorescence measurements can distinguish between covalent and non-covalent binding modes.

The intrinsic fluorescence of the acridine label can be used for the detection of acridinylated prion protein in a poly(acrylamide) gel (Figs. 4, 5). Free quinacrine is visible as a strong band at the bottom of the gel using a UV transilluminator. The reduced form of the prion protein is also visible on a transilluminator after treatment with quinacrine, whereas the prion protein in the negative control sample without quinacrine treatment is not visible. For comparison, both labeled and unlabeled prion proteins were also visualized by staining with Coomassie blue. Since BSA contains an odd number of Cys residues, the

presence of a free SH group can also be visualized by quinacrine. Interestingly, in contrast to the oxidized form of glutathione, the oxidized form of the prion protein is stained by quinacrine on the gel. This might be explained by the presence of incompletely oxidized prion protein and by the redox properties of the full-length prion protein molecule, which normally binds a molecule of  $\text{Cu}^{2+}$  at its N-terminus (the octarepeat region, PrP51-91) and is capable of reducing copper (II) to copper (I) (Nadal et al. 2007). Thus, quinacrine can serve as a staining agent for the free thiol groups of Cys-containing proteins.

### NMR spectra

The  $^1\text{H}$  and  $^{13}\text{C}$  chemical shifts were assigned using 2D COSY, HSQC and HMBC data (Supporting Information-2). The strong HMBC correlation between the hydrogens ( $\delta$  3.11, 3.35) and carbon ( $\delta$  139.3), and between hydrogens (3.14, 3.36) and carbon ( $\delta$  139.5) indicated that acridine moiety was attached to the sulfur of [Cys(Qui) $^{178}$ ]MoPrP177-180 (**3a**) and [Cys(Qui) $^{178}$ ]MoPrP176-180 (**3b**),

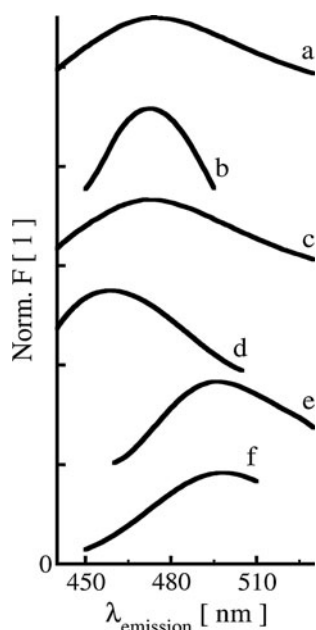


**Fig. 3** Normalized and smoothed fluorescence spectra recorded with an excitation wavelength of 269 nm: *a* the prion-derived peptide **3a**; *b* the prion-derived peptide **3b**; *c* the prion-derived peptide **3e**; *d* labeled rPrP **3g**; *e* quinacrine; and *f* a 1:2 mixture of rPrP and quinacrine

**Table 3** The parameters of the fluorescence spectra of selected compounds

Compound	Excitation maxima (nm)	Emission maximum (nm)
Quinacrine	280, 343, 425, 445	500
[Cys(Qui) $^{178}$ ]MoPrP177-180 ( <b>3a</b> )	267, 347, 363, 399, 417	474
[Cys(Qui) $^{178}$ ]MoPrP176-180 ( <b>3b</b> )	267, 363, 398, 417	473
[Cys(Qui) $^{178}$ , Asn $^{216}$ ]MoPrP210-216 ( <b>3e</b> )	267, 347, 363, 398, 417	471
HisTag-[Cys(Qui) $^{178,213}$ ]MoPrP23-230 ( <b>4g</b> )	269, 394, 413	459

respectively. A similar correlation between the hydrogens ( $\delta$  3.17, 3.28) and carbon ( $\delta$  139.3) confirmed the attachment of an acridine moiety to the Cys in [Cys(Qui) $^{213}$ , Asn $^{216}$ ]MoPrP210-216 (**3e**). In the glutathione derivative **3g**, a similar correlation between the hydrogens ( $\delta$  3.18 and 3.33) and carbon ( $\delta$  139.4) also provided evidence for attachment of an acridine moiety to the sulfur atom.

### Mass spectra

Because of the inaccuracy of MALDI-TOF measurements, samples of recombinant (**2g**) and labeled recombinant (**4g**) prion proteins were analyzed with deconvolution empowered Q-ToF ESI (see Supporting Information-4). The molecular weight of the labeled protein **4g** was about  $484 \pm 7$  Da higher than that of the unlabeled prion protein (**2g**). This mass difference corresponds to the monoisotopic molecular weight of two acridine units from quinacrine (484.07 Da for  $\text{C}_{28}\text{H}_{18}\text{N}_2\text{O}_2\text{Cl}_2$ , or 482.06 Da when two hydrogens have been lost). In the case of the prion peptide **2f**, the prolonged acridinylation to **4f** increased the molecular weight by about  $482.1 \pm 0.9$  Da. Again, the increase corresponds to two acridine units. This result suggests that the prion protein **2g** and prion-derived peptides **2a**, **2b** and **3d–2f** can accept up to two acridine units (**4a**, **4b** and **4d–4g**), which positively correlates with the number of Cys residues in the amino acid sequence. The only exception to this was peptide **2b**, which contains an N-terminal His residue.

### Trypsin map

The full-length protein **2g** and its labeled analog **4g** were cleaved with trypsin. The peptide maps obtained were compared using MALDI-MS. For the labeled prion protein, five important fragments—[Cys(Qui) $^{178}$ ]MoPrP156-193 (**6a**), [Cys(Qui) $^{178}$ ]MoPrP156-203 (**6b**), [Cys(Qui) $^{178}$ ]MoPrP151-203 (**6c**), [Cys(Qui) $^{178,213}$ ]MoPrP156-219 (**6d**) and [Cys(Qui) $^{178,213}$ ]MoPrP156-228 (**6e**), (see Supporting Information-3)—were identified. The difference in mass corresponds to the Qui unit that has lost hydrogen and is close to the masses of the dipeptides: His-Cys, Cys-His, Ile-Lys, Lys-Ile, Lys-Leu, Leu-Lys, Ile-Gln, Gln-Ile, Leu-Gln and Gln-Leu. Fortunately, none of these dipeptides are adjacent to the trypsin cleavage sites. No acridinylation

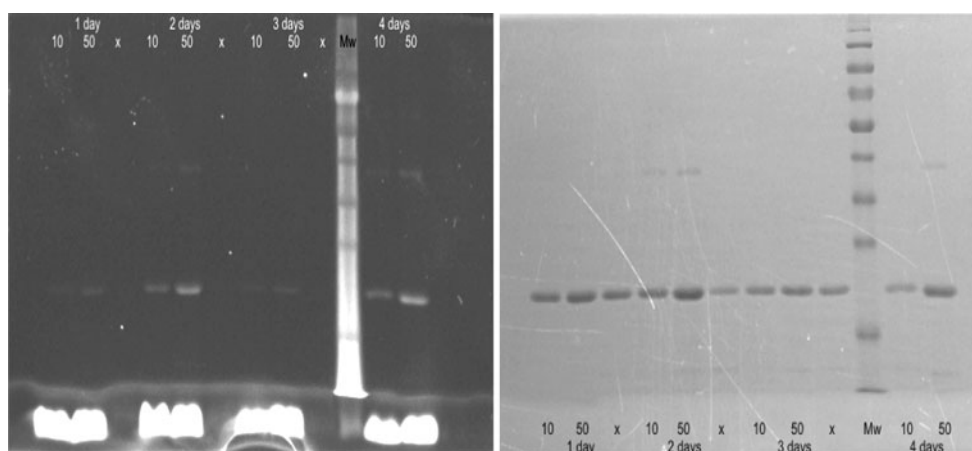


**Fig. 4** PAGE-electrophoresis of oxidized recombinant HuPrP (**2g**) after incubation with 10, and 50 or 0  $\mu\text{M}$  quinacrine; marked as 10, 50 and x, respectively. The *left panel* was obtained by transillumination with UV light, the *right one* was obtained by staining with Coomassie brilliant blue

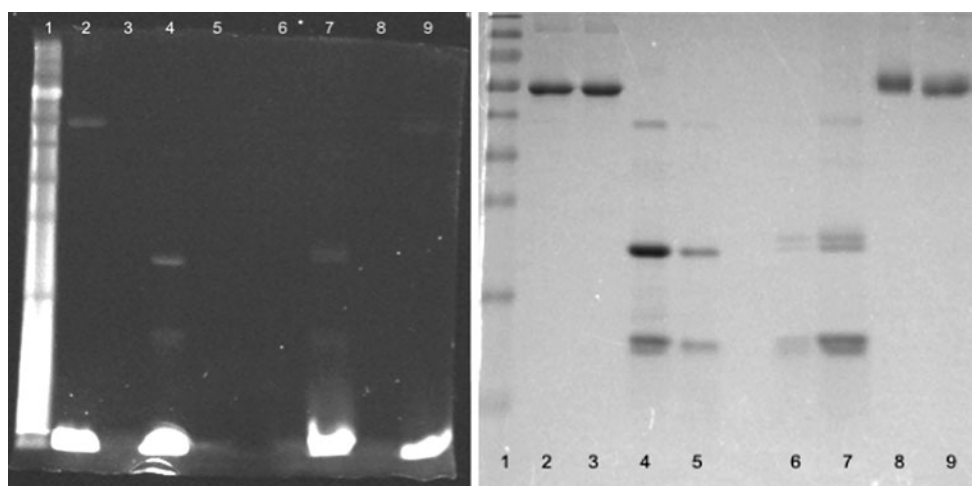


**Fig. 5** PAGE-electrophoresis of bovine serum albumin (BSA) and recombinant HuPrP (**2g**) with and without quinacrine (10  $\mu\text{M}$ ). Oxidized BSA was incubated in the presence (line 2) and absence (line 3) of quinacrine, as well as, oxidized recHuPrP (lines 4 and 5,

respectively), reduced recHuPrP (lines 7 and 6, respectively) and reduced BSA (lines 9 and 8, respectively). The *left panel* was obtained by transillumination with UV light, and the *right one* was obtained by staining with Coomassie brilliant blue

was observed for the N-domain fragments. All of the fragments containing the acridine moiety most likely correspond to domains containing one or two Cys residues.

#### Site of acridinylation

In this work, we have already shown by NMR (**3a–3g** and **4a–4g**) that the reactivity of amino acids such as Asp, Asn, Cys, Glu, His, Met, Gln, Thr and Thz with the quinacrine is limited to the thiol group of Cys and partially to the N-terminal amino group of His. The acridine label does not react with the Met sulfide group, in contrast to common labels based on alkylation reagents, such as alkyl halides or alkyl sulfates. In contrast to our previous observation of the labeling of  $\epsilon$ -amino groups of Lys residues in dipolar

aprotic solvents (Šebestík et al. 2006), the reactivity of the amino group is governed by its  $\text{p}K_{\text{a}}$  under aqueous conditions (Paul and Ladame 2009). Thus, under physiological aqueous conditions, Lys and Arg are not susceptible to acridinylation, which indicates that our previous model using an aprotic solvent as a protein environment is inadequate. It could be seen on bis-acridinylation of MoPrP178-213 (**4f**), which contains two Cys, one Arg, and three Lys residues. However, tris-, oligo- and poly-acridinylations were not observed using LC-MS. Moreover, the UV-vis spectrum of  $[\text{Cys}^{178,213}(\text{Qui})]\text{MoPrP178-213}$  (**4f**, Figs. 2, 3) also agrees with the mono-acridinylated species (**3a–3f**). Therefore, we suggest that the site of prion protein acridinylation is the thiol group of Cys, which is consistent with the thiol groups having the highest

nucleophilicity relative to the other functional groups found in peptides and proteins. In the case of the prion protein, the labeling exclusively led up to formation of the bis-acridinylated species, which correlates well with the presence of two Cys residues in the protein molecule. The fluorescence spectrum of the labeled prion protein (**4g**) is also similar to those of the prion peptides **3a–3c** labeled at a thiol group. Because quinacrine selectively reacts with the thiol group, but leaves the disulfide linkage unaffected in a non-reductive environment, this approach can be used for the in vitro labeling of free thiol groups. It appears that PrP reacts with quinacrine, leading to the acridinylation of both thiol groups of the prion protein. Unlike alkylation agents based on alkyl halides, acridinylation does not affect the methionine side chains. Such acridinylation, which introduces fluorescence and absorbance in the visible region of UV–vis spectra, allows for the selective labeling of the thiol groups. If this reaction interferes with disulfide-bond formation, it can significantly influence prion diseases. The same positive influence might also occur with other 9-aminoacridines.

#### Summary of quinacrine reactivity

There are at least two discrepancies connected with the quinacrine mode of action. The first one is related to the difference between the high anti-prion activity of quinacrine in vitro (Korth et al. 2001) and its weak affinity for prion-protein molecule (Vogtherr et al. 2003). The ratio between  $K_d$  and  $EC_{50}$  is 15,333; in other words, quinacrine is almost four orders of magnitude more active than its activity would be estimated to be from the dissociation constant. When prion protein (**2g**) is bis-acridinylated, as it was observed to be in this work, a synergistic anti-prion effect could be achieved. As shown on smaller models, two acridine units must be at a proper distance ( $\sim 10 \text{ \AA}$ ) (May et al. 2003). This finding could explain the enhancement of the quinacrine anti-prion effect.

The second discrepancy is related to the difference between the high activity of quinacrine in vitro and its failure to have a therapeutic effect in vivo. The reaction of glutathione with quinacrine has previously been observed (Wild and Young 1965). Here, we have fully characterized its product (**4h**), which suggests that glutathione competes with the prion protein. In the in vitro neuronal cell cultures, the extracellular concentration of glutathione is kept very low (maximum of  $3 \mu\text{M}$ ), whereas the glutathione concentration in plasma and other human compartments is significantly higher (approximately  $12 \text{ mM}$ ) (Dringen 2000). Therefore, in the in vivo assays, quinacrine has to survive a concentration of glutathione approximately four orders of magnitude higher than in the in vitro studies,

which may explain quinacrine's lack of efficacy during clinical trials.

#### Conclusions

We have performed a series of reactions between quinacrine and model peptide and protein systems. Our results strongly suggest that the acridine moiety of quinacrine can be transferred to mouse recombinant prion protein and the prion-derived peptides. The thiol groups of the peptides and proteins function as binding sites and selectively capture the acridine moiety, as was determined from the spectroscopic experiments. In particular, the acridinylated prion protein and prion-derived peptides could be easily distinguished on the basis of the UV–vis and fluorescence spectra. The selective reaction of quinacrine with thiols thus provides an excellent tool for labeling free thiol groups in proteins. This reaction does not affect other groups, except for thiols and N-terminal amino groups in close proximity to imidazole and thiol groups.

The moderate reactivity of the prion thiols indicates that a quinacrine-based drug could probably modify prion aggregates. Unfortunately, quinacrine can be scavenged by a thiol group of glutathione in vivo, which is a plausible explanation for the lack of quinacrine activity in clinical trials.

**Acknowledgments** This work was supported by the Czech Science Foundation (GA CR) Grant No. 203/07/1517. KH, OJ and ED were supported by the projects of Charles University in Prague: PRVOUK-P24/LF1/3, UNCE 204022 and SVV-2012-264506. English language revision was made by American Journal Experts, <http://www.journal-experts.com>.

**Conflict of interest** Authors declare that they have no conflict of interest.

#### References

- Bolognesi ML, Cavalli A, Valgimigli L, Bartolini M, Rosini M, Andrisano V, Recanatini M, Melchiorre C (2007) Multi-target-directed drug design strategy: from a dual binding site Acetylcholinesterase inhibitor to a trifunctional compound against Alzheimer's disease. *J Med Chem* 50:6446–6449
- Burnett JC, Schmidt JJ, Stafford RG, Panchal RG, Nguyen TL, Hermone AR, Vennerstrom JL, McGrath CF, Lane DJ, Sausville EA, Zaharevitz DW, Gussio R, Bavari S (2003) Novel small molecule inhibitors of Botulinum neurotoxin. A metalloprotease activity. *Biochem Biophys Res Commun* 310:84–93
- Chang CD, Waki M, Ahmad M, Meienhofer J, Lundell EO, Haug JD (1980) Preparation and properties of *N*-9-fluorenylmethoxycarbonylamino acids bearing tert-butyl side chain protection. *Int J Pept Prot Res* 15:59–66

- Claude S, Lehn JM, Vigneron JP (1989) Bicyclo-bis-intercalands: synthesis of triply bridged bis-intercalands based on acridine subunits. *Tetrahedron Lett* 30:941–944
- Cobb NJ, Surewicz WK (2009) Prion diseases and their biochemical mechanisms. *Biochemistry* 48:2574–2585
- Collinge J, Gorham M, Hudson F, Kennedy A, Keogh G, Pal S, Rossor M, Rudge P, Siddique D, Spyer M, Thomas D, Walker S, Webb T, Wroe S, Darbyshire J (2009) Safety and efficacy of quinacrine in human prion disease (PRION-1 study): a patient-preference trial. *Lancet Neurol* 8:334–344
- Collins SJ, Lewis V, Brazier M, Hill AF, Fletcher A, Masters CL (2002) Quinacrine does not prolong survival in a murine Creutzfeldt-Jakob Disease model. *Ann Neurol* 52:503–506
- Demeunynck M, Charmantray F, Martelli A (2001) Interest of acridine derivatives in the anticancer chemotherapy. *Curr Pharm Des* 7:1703–1724
- Denny WA (2003) Acridine-4-carboxamides and the concept of minimal DNA intercalators. In: Demeunynck M, Bailly C, Wilson WD (eds) *In small molecule DNA and RNA binders*. Wiley-VCH Verlag GmbH & Co, Weinheim, pp 482–502
- Dollinger S, Lober S, Klingenstein R, Korth C, Gmeiner PA (2006) Chimeric ligand approach leading to potent antiprion active acridine derivatives: design, synthesis, and biological investigations. *J Med Chem* 49:6591–6595
- Dondi F (1982) Approximation properties of the Edgeworth-Cramer series and determination of peak parameters of chromatographic peaks. *Anal Chem* 54:473–477
- Dringen R (2000) Metabolism and functions of glutathione in brain. *Progress Neurobiol* 62:649–671
- Eiter LC, Hall NW, Day CS, Saluta G, Kucera GL, Bierbach U, Gold I (2009) Analogues of a platinum-acridine antitumor agent are only moderately cytotoxic but show potent activity against *Mycobacterium tuberculosis*. *J Med Chem* 52:6519–6522
- Fields GB, Noble RL (1990) Solid phase peptide synthesis utilizing 9-fluorenylmethoxycarbonyl amino acids. *Int J Pept Prot Res* 35:161–214
- Flavell RR, Huse M, Goger M, Trester-Zedlitz M, Kuriyan J, Muir TW (2002) Efficient semisynthesis of a tetraphosphorylated analogue of the type I TGF $\beta$  receptor. *Org Lett* 4:165–168
- Franks NP, Abraham MH, Lieb WR (1993) Molecular-organization of liquid n-octanol: an X-ray diffraction analysis. *J Pharm Sci* 82:466–470
- Gaydukevich AN, Kazakov GP, Kravchenko AA, Porokhnyak LA, Pinchuk VV, Velikii DL (1987) Synthesis and biological activity of acridinyl-9-thioacetic acids and their derivatives. *Pharm Chem J* 21:633–636
- Ghaemmaghami S, Ahn M, Lessard P, Giles K, Legname G, DeArmond SJ, Prusiner SB (2009) Continuous Quinacrine treatment results in the formation of drug-resistant prions. *PLoS Pathogens* 5: art no e1000673
- Goodell JR, Ougolkov AV, Hiasa H, Kaur H, Rimmel R, Billadeau DD, Ferguson DM (2008) Acridine-based agents with Topoisomerase II activity inhibit pancreatic cancer cell proliferation and induce apoptosis. *J Med Chem* 51:179–182
- Guddneppanavar R, Saluta G, Kucera GL, Bierbach U (2006) Synthesis, biological activity and DNA-damage profile of platinum-threading intercalator conjugates designed to target adenine. *J Med Chem* 49:3204–3214
- Kaiser E, Colescot RL, Bossinger CD, Cook PI (1970) Color test for detection of free terminal amino groups in the solid-phase synthesis of peptides. *Anal Biochem* 34:595–598
- Korth C, May BCH, Cohen FE, Prusiner SB (2001) Acridine and phenothiazine derivatives as pharmacotherapeutics for prion disease. *Proc Natl Acad Sci USA* 98:9836–9841
- Krauth-Siegel RL, Bauer H, Schirmer H (2005) Dithiol proteins as guardians of the intracellular redox milieu in parasites: old and new drug targets in trypanosomes and malaria-causing plasmodia. *Angew Chem Int Ed* 44:690–715
- Krchňák V, Vágner J, Lebl M (1988a) Non-invasive continuous monitoring of solid-phase peptide synthesis by acid-base indicator a. *Int J Pept Prot Res* 32:415–416
- Krchňák V, Vágner J, Šafař P, Lebl M (1988b) Non-invasive continuous monitoring of solid phase peptide synthesis by acid-base indicator b. *Collect Czech Chem Commun* 33:2542–2548
- Kunikowski A, Ledochowski A (1981) Reactions at C9 of acridine-derivatives 28. Kinetics of hydrolysis of N-(1-nitroacridyl-9)-D,L-amino acids. *Polish J Chem* 55:1979–1984
- Lehn JM (1993) Supramolecular chemistry. *Science* 260:1762–1763
- Lewis JS (1949) The N-acylation of N-(4-methoxyphenyl)-4-chloro-anthranilic acid. *J Org Chem* 14:285–288
- Madden HH (1978) Comments on the Savitzky-Golay convolution method for least-squares fit smoothing and differentiation of digital data. *Anal Chem* 50:1383–1386
- May BCH, Fafarman AT, Hong SB, Rogers M, Deady LW, Prusiner SB, Cohen FE (2003) Potent inhibition of scrapie prion replication in cultured cells by bis-acridines. *Proc Natl Acad Sci USA* 100:3416–3421
- Meienhofer J, Waki M, Heimer EP, Lambros TJ, Makofske RC, Chang CD (1979) Solid phase synthesis without repetitive acidolysis. Preparation of leucyl-alanyl-glycyl-valine using 9-fluorenylmethoxycarbonylamino acids. *Int J Pept Prot Res* 13:35–42
- Nadal RC, Abdelraheim SR, Brazier MW, Rigby SEJ, Brown DR, Vile JH (2007) Prion protein does not redox-silence Cu<sup>2+</sup>, but is a sacrificial quencher of hydroxyl radicals. *Free Radical Biol Med* 42:79–89
- Orzáez M, Mondragon L, Garcia-Jareno A, Mosulen S, Pineda-Lucena A, Perez-Paya E (2009) Deciphering the antitumoral activity of Quinacrine: binding to and inhibition of Bcl-xL. *Bioorg Med Chem Lett* 19:1592–1595
- Paul A, Ladame S (2009) 9-Amino acridines undergo reversible amine exchange reactions in water: implications on their mechanism of action in vivo. *Org Lett* 11:4894–4897
- Pavliček A, Bednárová L, Holada K (2007) Production, purification and oxidative folding of the mouse recombinant prion protein. *Folia Microbiol* 52:391–397
- Phuan PW, Zorn JA, Safar J, Giles K, Prusiner SB, Cohen FE, May BCH (2007) Discriminating between cellular and misfolded prion protein by using affinity to 9-aminoacridine compounds. *J General Virol* 88:1392–1401
- Rodriguez-Franco MI, Fernandez-Bachiller MI, Perez C, Hernandez-Ledesma B, Bartolome B (2006) Novel tacrine-melatonin hybrids as dual-acting drugs for Alzheimer disease, with improved acetylcholinesterase inhibitory and antioxidant properties. *J Med Chem* 49:459–462
- Ronga L, Palladino P, Costantini S, Facchiano A, Ruvo M, Benedetti E, Ragone R, Rossi F (2007) Conformational diseases and structure-toxicity relationships: lessons from prion-derived peptides. *Curr Prot Pept Sci* 8:83–90
- Rosini M, Simoni E, Bartolini M, Cavalli A, Ceccarini L, Pascu N, McClymont DW, Tarozzi A, Bolognesi ML, Minarini A, Tumiatti V, Andrisano V, Mellor IR, Melchiorre C (2008) Inhibition of Acetylcholinesterase, beta-Amyloid aggregation, and NMDA receptors in Alzheimer's disease: a promising direction for the multi-target-directed ligands gold rush. *J Med Chem* 51:4381–4384
- Saravanamuthu A, Vickers TJ, Bond CS, Peterson MR, Hunter WN, Fairlamb AH (2004) Two interacting binding sites for quinacrine derivatives in the active site of trypanothione reductase. A template for drug design. *J Biol Chem* 279:29493–29500
- Sarin VK, Kent SBH, Tam JP, Merrifield RB (1981) Quantitative monitoring of solid phase peptide synthesis by the ninhydrin reaction. *Anal Biochem* 117:147–157

- Savitzky A, Golay MJE (1964) Smoothing and differentiation of data by simplified least squares procedures. *Anal Chem* 36:1627–1639
- Schantl JG, Türk W (1990) Synthesen von 1-(9-acridinyl)-3-hydroxyharnstoff und 9-acridanon-oxim. *Arch Pharm* 323:720–726
- Šebestík J, Šafařík M, Stibor I, Hlaváček J (2006) Acridin-9-yl exchange: a proposal for the action of some 9-aminoacridine drugs. *Biopolymers* 84:605–614
- Šebestík J, Hlaváček J, Stibor I (2007) A role of the 9-aminoacridines and their conjugates in a life science. *Curr Prot Pept Sci* 8:471–483
- Spilman P, Lessard P, Sattavat M, Bush C, Tousseyn T, Huang EJ, Giles K, Golde T, Das P, Fauq A, Prusiner SB, DeArmond SJ (2008) A  $\gamma$ -secretase inhibitor and quinacrine reduce prions and prevent dendritic degeneration in murine brains. *Proc Natl Acad Sci USA* 105:10595–10600
- Steinier J, Termonia Y, Deltour J (1972) Comments on smoothing and differentiation of data by simplified least square procedure. *Anal Chem* 44:1906–1909
- Tompa P, Tusnady GE, Friedrich P, Simon I (2002) The role of dimerization in prion replication. *Biophys J* 82:1711–1718
- Vogtherr M, Grimme S, Elshorst B, Jacobs DM, Fiebig K, Griesinger C, Zahn R (2003) Antimalarial drug quinacrine binds to C-terminal helix of cellular prion protein. *J Med Chem* 46:3563–3564
- Vojkovský T (1995) Detection of secondary amines on solid phase. *Pept Res* 8:236–237
- Wallace DJ (1989) The use of quinacrine (Atabrine) in rheumatic diseases—a reexamination. *Semin Arthritis Rheum* 18:282–297
- Weltrowski M, Ledochowski A, Sowinski P (1982) Research on tumor-inhibiting compounds 70. Reactions of 1-nitroacridines with ethanethiol. *Polish J Chem* 56:77–82
- Wild F, Young JM (1965) The reaction of Mepacrine with thiols. *J Chem Soc*, 7261–7274. doi:10.1039/JR9650007261
- Wille H, Bian W, McDonald M, Kendall A, Colby DW, Bloch L, Ollesch J, Borovinskiy AL, Cohen FE, Prusiner SB, Stubbs G (2009) Natural and synthetic prion structure from X-ray fiber diffraction. *Proc Natl Acad Sci USA* 106:16990–16995
- Wysocka-Skrzela B (1986) Research on tumor inhibiting compounds. Part LXXVI. Reactions of 1-nitro-9-aminoacridine derivatives, new antitumor agents with nucleophiles. *Polish J Chem* 60:317–318
- Yamamoto T, Miller WH (2005) Path integral evaluation of the quantum instanton rate constant for proton transfer in a polar solvent. *J Chem Phys* 122:art no 044106
- Yung L, Huang PY, Lessard P, Legname G, Lin ET, Baldwin M, Prusiner SB, Ryou C, Guglielmo BJ (2004) Pharmacokinetics of Quinacrine in the treatment of prion disease. *BMC infectious diseases* 4:art no 53
- Zawada Z, Šebestík J, Šafařík M, Krejčířková A, Březinová A, Hlaváček J, Stibor I, Holada K, Bouř P (2010) What could be the role of Quinacrine in Creutzfeldt–Jakob Disease treatment? In: Lebl M, Meldal M, Jensen K, Hoeg-Jensen T (eds) *Peptides 2010. Proc 31st Eur Pep Symp. Eur Pep Soc, Copenhagen*, pp 84–85
- Zawada Z, Šebestík J, Šafařík M, Bouř P (2011) Dependence of the reactivity of acridine on its substituents: a computational and kinetic study. *Eur J Org Chem* 2011:6989–6997